DETERMINATION OF HEAT PRODUCTION ZONES AT OPEN-CAST MINE DUMP

By M. Schreck,[1] Associate Member, ASCE, M. Nishigaki,[2] Member, ASCE, H.-R. Gläser,[3] G. Christoph,[4] S. Großwig,[5] E. Hurtig,[6] M. Kasch,[7] and K. Kühn[8]

ABSTRACT: The chemical processes and their thermal effects taking place inside a dump of an open-cast mine during a reclamation process are a matter of interest among geoenvironmental engineers and scientists. Fiber-optic-distributed-temperature sensing (DTS) was applied together with a soil ground water monitoring system (SGM-System) at the dump in the open-cast mine (Cospuden) for investigating those processes. An optical fiber was mounted at the entire length of a double-pipe SGM-System. The temperature was measured monthly, along the depth of 50 m, with a spatial resolution of 0.5 m. The accuracy of the temperature gauge was 0.05 K. The system was utilized for the localization of heat production zones in the subsurface, for the determination of the temperature variation's penetration depth from the surface into the soil of the dump and for the determination of the influence of the SGM-System on the subsurface temperature balance. The results were compared with a heat transport model and then interpreted.

INTRODUCTION

Large open-cast mine areas are situated in parts of central and eastern Germany. At the present time, the fast and efficient reclamation of these areas after the mines' resources have been depleted is a problem facing engineers and scientists. In cooperation with other research groups, the UFZ (Center for Environmental Engineering Research Leipzig-Halle) has been studying the hydrochemical and geochemical processes at the idle open-cast mine, Cospuden.

One of the topics of the research program deals with the possibility of determining the location of chemical active reaction zones and, it has been argued, that active reaction zones cause an increase in temperature of approximately 4 K (Ahead and Bobba 1971; Sigg and Stumm 1989; Merkel and Sperling 1996).

Pyrite:

$$FeS_2 + 3\frac{1}{2}O_2 + H_2O \rightarrow Fe^{2+} + 2SO_4^{2-} + 2H^+ + 1{,}448\ \text{kJ/mol} \quad (1)$$

Organic carbon:

$$C_6H_{12}O_6 + 6O_2 \rightarrow 6CO_2 + 6H_2O + 2{,}822\ \text{kJ/mol} \quad (2)$$

The main question was whether these zones could be identified by their heat effect on the subsurface. For maintaining the problem the following solution strategy was developed. Variations in temperature distribution in the subsurface are caused through the following effects:

- (A) Temperature variations at the surface through vertical heat penetration.
- (B) Internal heat production sources.
- (C) Heat transport through ground water flow.
- (D) Heat transport from the dump side surface.

The vertical penetration of heat from the surface into an unsaturated subsurface (A) can be described by a vertical one-dimensional (1D) heat transfer model. If it is possible to determine the vertical distribution of temperature in the subsurface with a high spatial resolution and high accuracy and without any impact on the subsurface through the monitoring process, the comparison of the data obtained and the data of such a model would enable the possibility to determine the location and quantity of the sum of (B) + (C) + (D).

For this purpose, a soil ground water monitoring system (SGM-System) was extended with a fiber-optic-distributed-temperature sensing system (DTS-System) and installed on the dump of the remaining pit. Thus it was possible to determine the vertical temperature distribution of the soil body and to take depth-oriented water examinations without a further disturbance on the subsurface through the monitoring process after the system was installed. The temperature was measured monthly with a spatial resolution of 0.5 m in the 50-m deep borehole. The monitoring was undertaken from February 1995 until July 1996.

The results derived from the fiber-optic DTS-System are then compared with those of a 1D vertical heat transport model. The separation of soil influencing temperature processes from the natural temperature distribution inside the borehole of the SGM-System was conducted and the obtained results are presented in this paper.

AREA OF INVESTIGATION

The area under investigation is located in the south of the city of Leipzig in the Weißelsterbecken (River Elster basin) where a considerable number of open-cast mines have been closed down since 1990. In most cases, the reclamation program provides for the idle pits to be flooded. One of these former open-cast mines is the remaining pit at Cospuden, which is currently being flooded; the pit was closed down in 1992. A double seam of the Eocene and the Oligocene Epochs used to be mined here. In terms of facies, the upper lying Tertiary rock can be subdivided into a terrestrial and a marine complex. Glauconite, montmorillonite, quartz, calcite, and pyrite predominate in the coarse clay and sands have been differentiated. The selected area under investigation is a 2-km^2

---

[1] Okayama Univ., 1-1, Naka 1-chome, Dept. of Envir. Engrg., Okayama 700, Japan. E-mail: martin@cc.okoyama-u.ac.jp.

[2] Okayama Univ., 1-1, Naka 1-chome, Dept. of Envir. Engrg., Okayama 700, Japan. E-mail: martin@cc.okayama-u.ac.jp.

[3] Ctr. for Envir. Res. Leipzig/Halle, Hallesche Strasse 44, 06246 Bad Lauchstädt, Germany.

[4] Ctr. for Envir. Res. Leipzig/Halle, Hallesche Strasse 44, 06246 Bad Lauchstädt, Germany.

[5] GESO GmbH, Jena, Max-Gräfe-Gasse 10, 07743 Jena, Germany.

[6] GESO GmbH, Jena, Max-Gräfe-Gasse 10, 07743 Jena, Germany.

[7] GESO GmbH, Jena, Max-Gräfe-Gasse 10, 07743 Jena, Germany.

[8] GESO GmbH, Jena, Max-Gräfe-Gasse 10, 07743 Jena, Germany.

Note. Editor: Byung R. Kim. Discussion open until December 1, 1998. To extend the closing date one month, a written request must be filed with the ASCE Manager of Journals. The manuscript for this paper was submitted for review and possible publication on October 3, 1997. This paper is part of the ***Journal of Environmental Engineering***, Vol. 124, No. 7, July, 1998. ©ASCE, ISSN 0733-9372/98/0007-0646–0651/$8.00 + $.50 per page. Paper No. 16734.

TABLE 1. Sulphide and Organic Carbon with Respect to Depth

Depth (m) (1)	Sulphide (mass %) (2)	Organic carbon (mass %) (3)
2	0.49	9.19
6	0.14	2.26
12	0.47	8.68
14	0.78	14.73
16	0.62	12.87
17	0.07	1.68
18	0.15	1.01
20	0.43	0.90
24	0.90	0.81
27	0.60	0.55
28	0.68	0.82
48	0.87	1.15

part circumventing the dump. The starting point for the SGM borehole is located on the lakeside edge of the dump in the open-cast mine. In mining terms, this dump can be subdivided into two distinct sections: firstly the area known as the conveyor bridge dump, mainly containing the spoil removed from the upper layer of the coal seam (marine silts and sands); secondly the spreader dump, where the sediment from between the two coal seams was mainly differentiated (essential river sands). The conveyor bridge is located within a depth of 60 to 90 m above sea level.

The maximum pyrite content of some layers of sediment at the dump is 0.7–0.8%. The distribution of the soil characteristic inside the dump is different. An analysis of the profile, carried out by Ruhr-University Bochum, shows that the sulphide content is lower than 1%, but in some layers, the organic n content is 12–15% (Table 1).

INSTALLATION OF SGM-DTS-SYSTEM

The SGM-DTS-System is used for depth-oriented hydrochemical water examination and for vertical distributed temperature sensing during the flooding process inside the body of the dump. The recording shaft of the SGM-System passes through the dump and stops at a depth of 50 m in the contact area where the pre-Tertiary stratum begins. The system is located within a dump valley structure. Here the four sampling horizons are completely covered by bulk material from the conveyor bridge dump; hence, they would have the highest contents of acid-producing minerals. The sampling hoses (1–4) of the SGM-System being used for taking depth-orientated water samples in the dump extend to the contact area of the pre-Tertiary stratum (Fig. 1). Detailed information about SGM-System are given in Luckner et al. (1991).

Due to the exothermic chemical reactions in the soil body of the dump, a DTS-System was mounted on the SGM-System. This combined system has some advantages compared to a conventional temperature measuring system, as follows (Schreck et al. 1997)

- Fast and precise gauge with high spatial resolution.
- No influence on the measured area by the measurement process.
- Long-time monitoring is easily possible.

The applied fiber-optic temperature sensing mechanism utilizes the Raman backscattering effect. The basic principle of the scattering mechanism needs a microscopic reflection of the effects. Coherent laser light enters the fiber and is transmitted through the fiber. In case of no impact on the fiber from the outside, low loss of light intensity occurs in the fiber (Schreck et al. 1997).

The temperature impact on the fiber changes the microscopic properties of the fiber and higher loss of laser light occurs on the output of the fiber. The loss occurring on the outcoming light intensity of the pulsed light beam is proportional to the temperature impact on the fiber. The location of the external disturbances along the fiber axis can be determined through time-reflected analysis of the backscattered light intensity. The physical principle of the sensing mechanism is presented in detail in (Hurtig et al. 1995).

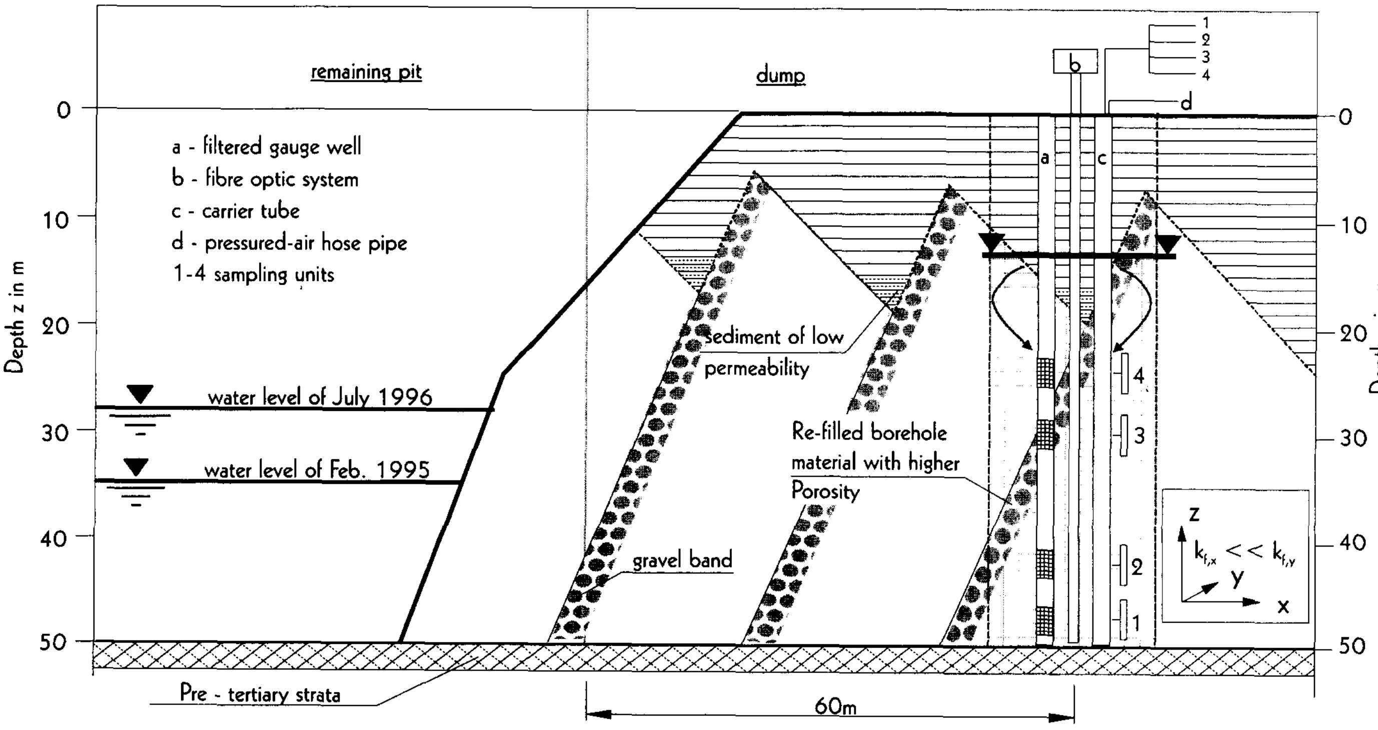

FIG. 1. Cross Section of Measured Profile (Schematically)

GEOPHYSICAL INVESTIGATION

The aim of the geophysical measurements was to describe inhomogeneities and the degree of water saturation inside the dump body to investigate hydrochemical reactions. It was found that the hydraulical phenomena inside the dump are very difficult. These circumstances complicated the interpretation of both temperature and geophysical response.

Ultimately, the water levels in the measuring pipes, in the remaining pit, and in the dump massif are not identical. The dump massif is only partially water saturated. Refraction seismic in the immediate vicinity of the SGM measured P-wave spreading velocities in the dump massif of up to only 600 m/s. This indicates incomplete water saturation in the dump material. However, this initially contradicts observations of the water level in the 2-in. measuring pipe, where a water level in a depth of about 14 m was found. It is currently believed that pore space drainage from the dump material to the SGM is taking place. It is also assumed that water from a perched water level is transmitted by gravel bands, immediately after drilling works (see Fig. 1). Dual-induction log measurements, taken in another gauge well, seem to back up these assumptions. Due to a defect in the filtered gauge well of the SGM-System, such logging could not be carried out. The geohydraulical interpretation results of geophysical investigations and the results of the vertical temperature monitoring are shown in a schematical cross section in Fig. 1. It is assumed, in this work, that the SGM-DTS System is embedded in a water barrel within the range of 14 m to the bottom.

TEMPERATURE SENSING

The data are derived from the fiber-optic DTS as shown in Fig. 2. The temperature distribution graphs show changes within a depth of 5–30 m, where the symmetric course of the graph turns into a right-inclined course. The temperature increases by 4 K at a depth of 5–11 m and decreases at a depth of 11–30 m (Fig. 2). At a depth of 14–50 m, increasing variations in temperature versus time and depth of 1 K have been (Fig. 3). It was found that heat variations caused at the surface in June 1995 and June 1996 can also be observed as an immediate variation in temperature at a depth of 14–50 m (Fig. 3).

Because there is no information about the temperature distribution at the location before the experiment started, it is not known whether the data obtained within the monitoring period are representative for the seasonal temperature variation. Therefore, the upper layer of the soil body of the dump should be ignored because it is influenced by daily temperature variations.

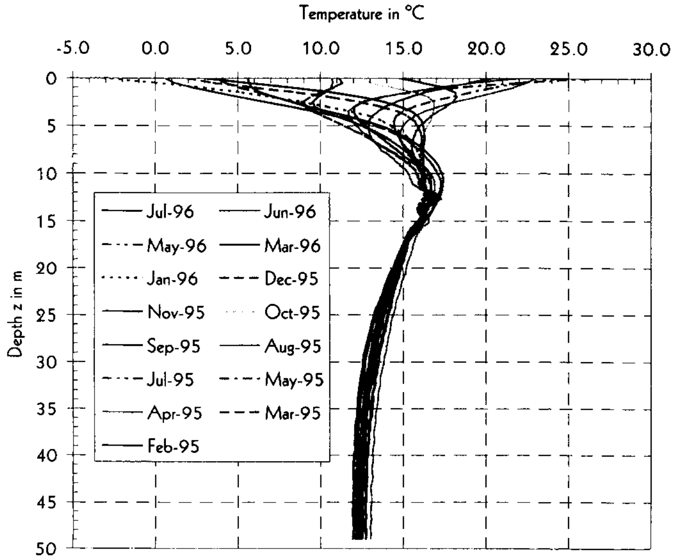

FIG. 2. Temperature Distribution versus Depth (February 1995–July 1996)

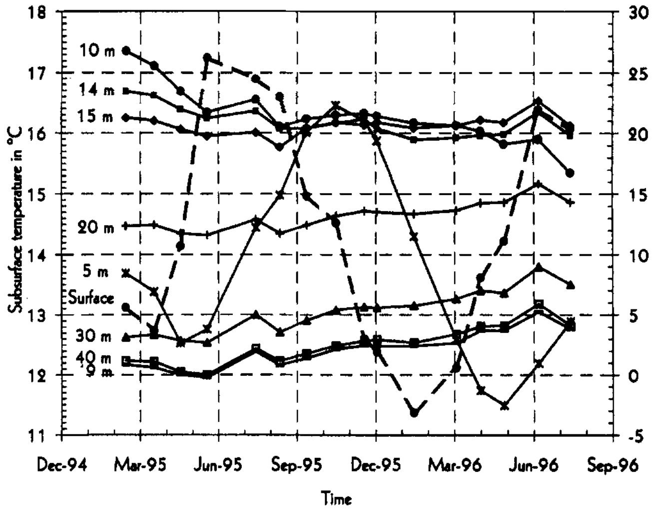

FIG. 3. Temperature Distribution Separated by Layers

For an initial estimation of the magnitude of the penetration depth l of daily and seasonal temperature variations from the surface into the soil body, an analytic equation presented in Kluge and Neugebauer (1986) was used. The temperature T at the depth z at time t is phase shifted to the temperature T_0 at time t at the surface. The phase shift is (Kluge and Neugebauer 1986)

$$\sqrt{\frac{\omega}{2\kappa}}\,z \tag{3}$$

If the maximal temperature on the surface is T_0 then the temperature in the depth z_l with a phase shift π is (Kluge and Neugebauer 1986)

$$-T_0 \exp - \sqrt{\frac{\omega}{2\kappa}}\,z_l \tag{4}$$

In this depth z_l the temperature is $T \sim T_0 \exp{-\pi} \sim 0.04T_0$, which is defined as the penetration depth l of seasonal temperature influence. So, the penetration depth l for the phase shift π is obtained with

$$l = \frac{\pi}{\sqrt{\frac{\omega}{2\kappa}}} \tag{5}$$

For porous unsaturated media (for first assumption $\kappa = 3 \times 10^{-7}$ m^2/s for unsaturated sand) (Marsily 1996), the penetration depth l for daily temperature influence is obtained to be 1 m and for seasonal temperature influence l is found to be 10 m (Kluge and Neugebauer 1986). Furthermore, it must be considered that a heat source can be situated at the monitoring location, inside the borehole itself or the heat can be transported through ground water flow from another source. Therefore the results of the geophysical investigation must be interpreted according to the zones of water saturation. The results of geohydraulic and geophysical investigations described earlier lead to the conclusion of an unsaturated soil in a depth less than 14 m. Therefore, the horizontal ground water flow and horizontal heat transfer are ignored in this layer. It was found that the increase in temperature at this layer must be caused through a heat source at the SGM-DTS System itself and the heat is not transferred from any other source.

MATHEMATICAL MODEL

Variations in temperature distribution in the subsurface are caused through temperature variations at the surface, additional internal heat sources, and ground water flow. The general equation for the heat transport through a porous medium is given by

$$\frac{\partial T}{\partial t} = -\Theta \frac{\rho_w \rho_s}{\rho c} v \cdot \nabla T + \nabla \lambda \cdot \nabla T + \kappa \nabla^2 T + \frac{\dot{Q}}{\rho_c} \qquad (6)$$

where $\rho c = \Theta \rho_w c_w + (1 - \phi)\rho_s c_s$ is the total heat capacity per volume; and $\kappa = \lambda/\rho c$ the thermal diffusivity. Due to the lack of horizontal flow and if at all weak seepage in the unsaturated substrate, we neglect the advective contribution. Furthermore, the system is assumed to be 1D along the vertical axis z. With these restrictions (6) simply reads

$$\frac{\partial T}{\partial t} = \frac{\kappa}{\lambda} \frac{\partial \lambda}{\partial z} \frac{\partial T}{\partial z} + \kappa \frac{\partial^2 T}{\partial z^2} + \frac{\dot{Q}}{\rho c} \qquad (7)$$

The interpretation of the measured temperature profile versus depth can be achieved by comparison with pure heat conduction, without any heat sources, i.e., $\dot{Q} = 0$

$$\frac{\partial T}{\partial t} = \frac{\kappa}{\lambda} \frac{\partial \lambda}{\partial z} \frac{\partial T}{\partial z} + \kappa \frac{\partial^2 T}{\partial z^2} \qquad (8)$$

The solutions of (8) for different times are then subtracted from the measured data. The remaining difference $\Delta T[\Delta T(z, t) = T_{\text{meas}} - T_{\text{calc}}]$ can be related to the heat source term $\dot{Q}$ of (9), which can be related to chemical reactions and heat transfer through ground water flow and seepage.

$$\dot{Q} = -\lambda \frac{\partial^2 \Delta T}{\partial^2 z^2} - \frac{\partial \lambda}{\partial z} \frac{\partial \Delta T}{\partial z} + \rho c \frac{\partial \Delta T}{\partial t} \qquad (9)$$

The numerical part is treated by standard techniques: First-order-accurate explicit time steps and central differences (Teukolsky et al. 1990) for the spatial derivatives.

CALIBRATION AND COMPUTATION OF MODEL

The difference of the phase shifting between the computed and the measured data for model calibration was compared. The model was calibrated by variation of thermal diffusivity κ and heat conductivity λ ($\rho \times c$ = const). Due to the assumption of an unsaturated subsurface at the dump, for model computation, changes of the parameter κ and λ versus depth have been neglected. Due to the calibration process, κ was determined to 5×10^{-7}m^2/s and λ to 2.5 W/m K over the depth. Those values correspond to wet sand ($\kappa = \lambda/\rho c$).

For the separation of daily temperature influences on the subsurface within the depth of 0–1 m, the graph of the temperature distribution at the level of 1 m was used as the time-dependent boundary condition for computation. The computation period of (5) to achieve a steady-state model condition was 10 years with the time-step-size of 0.1 day derived from a linear interpolation between two measured points. Therefore, only the data within a depth of 1 m $\leq z \leq$ 49 m have been taken into consideration for interpretation. Initial computation temperature was the temperature distribution of February 1995. The following questions needed to be answered.

1. What is the heat penetration depth l from the surface?
2. Where is/are the locations of heat production zones?
3. What caused the increase in temperature within the depth of 5–11 m?
4. What is the source for the increase in temperature within a depth of 14–49 m?

DISCUSSION

Penetration Depth of Temperature Variations at Surface

The penetration depth of temperature variations estimated earlier was proven by the results of the computing model using (5) (Fig. 4). At a depth of 10 m, the computation result shows a temperature variation less than 1 K. The frequency of computed data-graphs and measured data-graphs is identical, differences exist only in the elongation.

Heat Production Zones versus Depth

The separation of the natural temperature variations from additional temperature effects was obtained by subtracting computed data from monitored data (Fig. 5).

The heat production rate $\dot{Q}(z)$ was computed by using (6). The results are displayed in Fig. 4. Basically, it is shown that a heat production within a depth of 5–17 m is taking place. The maximum in heat production can be found at a depth of 11 m. The inner minimum between of 7 and 9 m results from special deposits of river sands without a high content of pyrite and organic carbon. This zone is also described as having less density by the radiometric borehole measurements.

It was discussed in Ritchie and Pantelis (1991) that con-

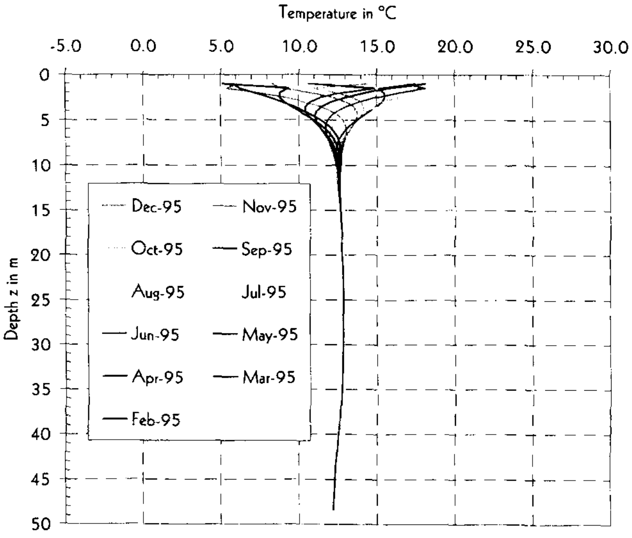

FIG. 4. Computation Results [by Using (5)]

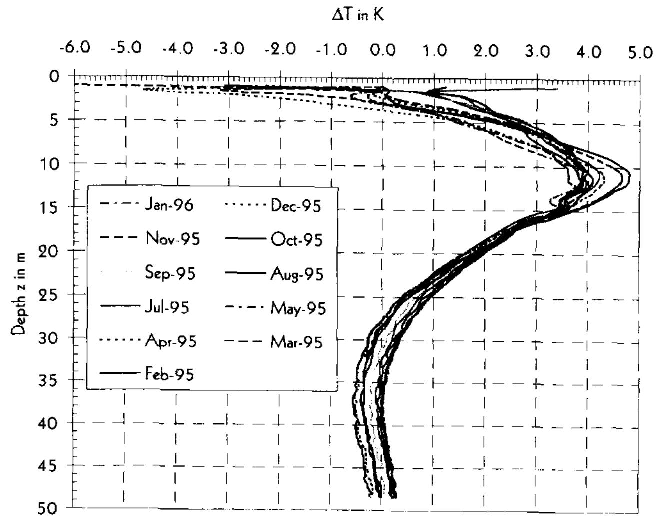

FIG. 5. Difference ΔT between Measured Data and Computed Data in K

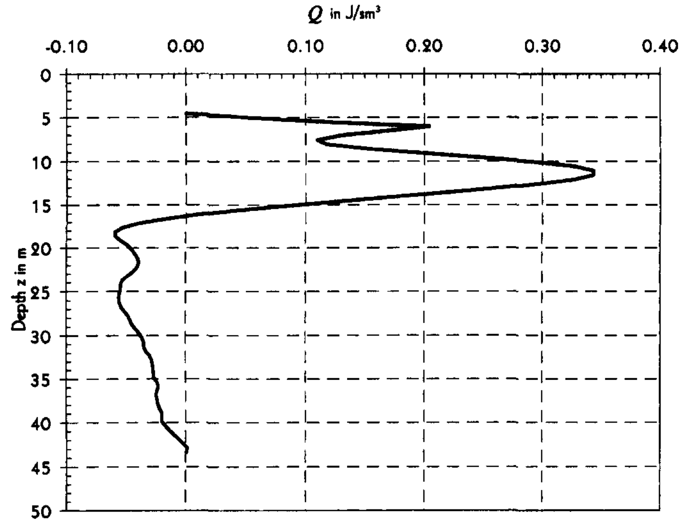

FIG. 6. Heat Production Rate in J/sm³

vection of air in the horizontal direction within the unsaturated layer of a waste dump provides a significant source of heat. Heat conductivity depends on the thermal conductivity of each phase, the structure of the solid matrix, the contact resistance, and gas convection at an unsaturated subsurface on the ratio of the mean free path and the average linear pore dimension (Kaviany 1995).

Oxygen migration with the fluid phase depends on the hydraulic conductivity and the decay rate. The dump consists of porous substrate—mainly marine silts and sands as well as river sands. The geophysical investigations have shown that the subsurface of the dump is unsaturated and not cracked. For the hydraulical conductivity and the inner structure of a conveyer bridge dump, Reichel and Uhlmann (1995) showed that the hydraulic conductivity of a mine dump is different because of the higher compaction and the demixing of the particles of the porous media due to the pour process. The hydraulic conductivity of the ripped structure of the conveyer bridge dump is mainly forming the geohydraulic conductivity of mine dumps (Reichel and Uhlmann 1995). Therefore, the subsurface of a mine dump has an anisotropy because the conductivity in a direction along the rib is higher than in a vertical direction to the rib $k_{f,x} << k_{f,y}$ (Fig. 1) (Reichel and Uhlmann 1995). The heating effect occurs only at a depth of 5–11 m and not along the whole depth. This effect can be explained with oxygen migration and pyrite oxidation via the gravel bands (Fig. 1), and it could be explained with heating effects from the dump side surface.

From the combined results of chemical analysis on the sediment samples (Table 1) and the results of the temperature measurement and its interpretation (Fig. 6) and (1) and (2), it can be concluded that the oxidation of organic carbon and pyrite could be the reason for the increase in temperature of up to 4 K within the depth range of 5–14 m.

Because of the high concentration of the reaction product sulphide and due to the decrease in temperature during the monitoring period within the depth of 5–15 m (Fig. 3), it is demonstrated that the previously described processes have been subsiding during the observation period.

Vertical Simultaneous Variation of Temperature versus Time within Depth of 14–50 m

The separation of temperature graphs by layers versus time (Fig. 3) might lead to the conclusion of a very fast heat penetration from the surface into the dump. The maximum temperature in July 1995 and June 1996 at the surface caused an immediate change of the soil temperature within a depth of 14–50 m. In contrast to this, Fig. 3 shows that the heat transfer in the soil is phase shifted over the depth within a depth of 0–10 m, and the amplitude of the temperature graph is subdued over depth and time. An explanation for this could be a heat conduction effect by the SGM-System, but this effect is not yet proven. An error of the temperature gauge could not be found. This matter will be the subject of future research.

CONCLUSIONS

The foregoing investigation has clearly demonstrated that the application of a DTS-System in conjunction with an SGM-System can improve existing information. The following conclusions may be drawn from this study.

- According to the monitored temperature effects and to the results of the chemical analysis (Table 1) of the water samples taken by the SGM-DTS System, oxidation of pyrite and organic sediments can explain the increase in temperature of 4 K.
- Heat production zones can be localized easier by the application of a fiber-optic distributed temperature measurement because temperature is a function of the chemical activity.
- The DTS-System enables the monitoring of the chemical reaction progress in conjunction with the examination of water samples taken by the SGM.
- The SGM-DTS System is a reasonable method for obtaining data to determine if a dump is undergoing oxidation. The method is useful in determining if measures taken to prevent oxidation are successful.
- The SGM-DTS System, or something along the SGM-DTS System, might be the reason for heat conduction. This effect is not clear and has to be investigated further.

The location of an SGM-System only delivers information about the SGM-System location and the immediate surroundings. This system needs to be applied to different locations on the bank of the remaining pit, and to investigate if it would be possible to monitor different locations of chemical active zones and interpret their results to protect the water body of the remaining pit against increasing acidification.

ACKNOWLEDGMENTS

Deutsche Forschungsgemeinschaft funded this research project. This work was done while the first writer was supported by the Ministry of Education of Japan and Deutscher Akademischer Austauschdienst (DAAD) Germany.

APPENDIX I. REFERENCES

Ahmad, M. V., and Bobba, A. C. (1971). "Temperature surveying of coal mines." *1st Int. Remote Sensing and Envir. Symp.*, Ann Arbor, Mich., 1109–1140.

Hurtig, E., et al. (1995). "Fiber optic temperature sensing: Application for subsurface and ground temperature measurements." *Tectonophysics*, 257, 101–109.

Kaviany, M. (1995). "Principles of heat transfer in porous media." *Mechanical engineers series.* Springer-Verlag KG, Berlin, 119.

Kluge, G., and Neugebauer, G. (1986). *Studienbücherei—grundlagen der thermodynamik.* VEB Deutscher Verlag für Wissenschaften, Berlin, 233.

Luckner, L., Nitsche, C., and Eichhorn, D. (1991). "Das SGM—system." *Die geowissenschaften.* Verlagsgesellschaft mbH Weinheim, 37–43.

Marsily, G. (1996). *Quantitative hydrology—groundwater hydrology for engineers.* Academic Press, Inc., Harcourt Brace Jovanovich, 277.

Merkel, B., and Sperling, B. (1996). "Hydrogeochemische stoffsysteme." *DVWK-Schriftenwerk,* 1(110), 1–288.

Reichel, F., and Uhlmann, W. (1995). "Wasserbeschaffenheit in tagebaurestseen." *Studien und tagungsberichte schriftenreihe des landes-*

umweltamt brandenburg, Berliner Strasse 21-25 14467, Potsdam, Germany, 6, 9–10.

Ritchie, A. I. M., and Pantelis, G. (1991). "Macroscopic transport mechanisms as a rate-limiting factor in dump leaching of pyritic ores." *Pollution abstracts, Appl. Math. Modeling*, 15(3), 136–143.

Schreck, M., et al. (1997). "Intrinsic fibre optic measurement—A new age of sensing?" *Sensormagazin*, Magazin Verlag, Jaegerweg 14, 31542 Bad Nenndorf, Germany, 4(4), 24–29.

Sigg, L., and Stumm, W. (1989). "Aquatische chemie." *Aquatische Chemie*, Zürich, 388.

Teukolsky, W. H., Vetterling, S. A., and Flannery, B. P. (1990). *Numerical recipes in C*, 2nd Ed., Cambridge University Press.

APPENDIX II. NOTATION

The following symbols are used in this paper:

c_s = specific heat capacity of substrate (J/kg K);
c_w = specific heat capacity of water (J/kg K);
k_f = hydraulic conductivity (m/s);
l = penetration depth (m);
$\dot{Q}$ = heat production rate (J/s m^3);
T = temperature (K);
v = fluid flux rate (m/s);
z = depth (m);
Θ = volumetric moisture content, $0 \leq \Theta \leq \phi$;
κ = thermal diffusivity (m^2/s);
λ = heat conductivity (W/m K);
ρ_s = mass density of substrate (kg/m^3);
ρ_w = mass density of water (kg/m^3);
ϕ = porosity; and
ω = frequency (l/s).

Subscripts

i = positive integer indices;
x = values in x-direction;
y = values in y-direction;
z = values in z-direction; and
0 = values at time t.